

Effect of temperature on compressive and tensile strengths of salt

Tanapol Sriapai, Chaowarin Walsri, Kittitep Fuenkajorn*

Geomechanics Research Unit, Institute of Engineering, Suranaree University of Technology, University Avenue, Muang District, Nakhon Ratchasima 30000 Thailand

*Corresponding author, e-mail: kittitep@sut.ac.th

Received 27 Dec 2011

Accepted 14 May 2012

ABSTRACT: A multi-axial strength criterion is developed to describe the distortional strain energy density of rock salt at failure as a function of the mean strain energy. The temperature effect on salt strength is implicitly considered by incorporating empirical relations between the elastic parameters and temperatures of the tested specimens. The proposed criterion agrees well with the test results obtained under temperatures ranging from 273–467 K. The proposed criterion is useful and practical for a conservative determination of the stability of compressed-air or gas storage caverns where the surrounding salt is subject to fluctuations of temperature during product injection and withdrawal periods.

KEYWORDS: strain energy, thermal effect, strength criterion, elasticity

INTRODUCTION

Temperature exerts an effect on deformability and strength of rocks^{1–3}. It has been found that rock strength and elastic properties decrease as the temperature increases. Rock salt studies on the temperature effect have focused on the time-dependent deformation (creep)^{4,5} where the results are specifically applied to assess the long-term performance of nuclear waste repositories in salt. Several complex formulations have been proposed to describe the thermo-mechanical behaviour of rock salt under the repository environment. Such formulations require several material parameters that are difficult to obtain, making their applications unpractical for the mining industry. In addition, experimental and theoretical studies on the effect of temperature on rock salt strength have been rare. Such knowledge is necessary for the design and stability analysis of salt around compressed-air and natural gas storage caverns⁶. During injection period a storage cavern may experience temperatures as high as 140 °C (414 K), depending on the injection rate and the maximum storage volume and pressure^{7–9}.

The objective of this study is to develop a multi-axial strength criterion for rock salt under various temperatures and confining pressures. The validity of the proposed criterion is verified by the results of uniaxial and triaxial compressive strength and Brazilian tensile strength tests on rock salt specimens subject to nominal temperatures of 273, 298, 404, and 467 K (0–194 °C). This selected range of testing

temperatures covers those likely occurred around the storage caverns under operation and gave a rigorous relationship between the temperatures and strengths of the salt.

Salt specimens

The salt specimens were prepared from 100 mm salt cores drilled from depths between 70 m and 100 m by Asean Potash Mining Co. in the Khorat basin, north-east Thailand. The salt cores belong to the Middle salt member of the Maha Sarakham formation¹⁰. The salt formation hosts several solution-mined caverns, and is considered as a host rock for compressed-air energy storage caverns by the Thai Department of Energy, and for chemical waste disposal by the Office of Atomic Energy for Peace^{11,12}. Fig. 1 shows a typical geologic section of the Maha Sarakham formation¹³. The formation was deposited 60–100 million years ago in the Cretaceous to early Tertiary ages¹⁴.

The salt cores tested here are virtually pure halite with average grain (crystal) sizes of $5 \times 5 \times 10$ mm³. For the compression testing, the cores were dry-cut to obtain cubical shaped specimens with nominal dimensions of $5.4 \times 5.4 \times 5.4$ cm³. The Brazilian test specimens were machined using a lathe to obtain 48 mm diameter circular disks with a thickness of 24 mm. No bedding is observed in the specimens.

To test the salt specimens under elevated temperatures, the prepared specimens and loading platens were heated in an oven for 24 h before testing. The low temperature specimens were prepared by cooling

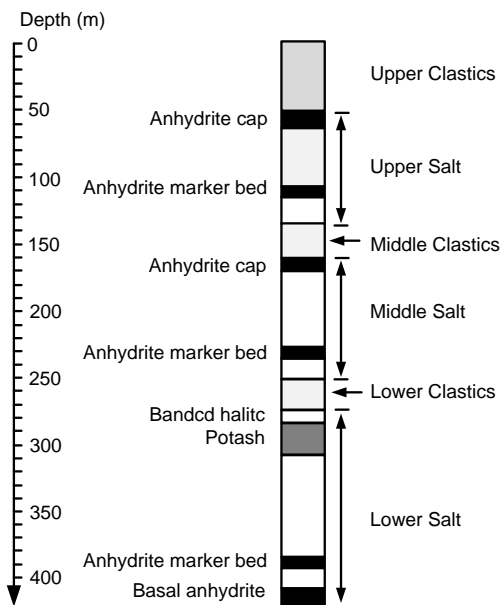


Fig. 1 A typical section of the Maha Sarakham formation¹³.

them in a freezer for 24 h. The mechanical testing is performed immediately after removing the samples from the oven or freezer. The specimen installation, equipment setup, and loading are completed within 4 min. The changes of specimen temperatures between before and after testing are less than 5 K. As a result the specimen temperatures are assumed to be uniform and constant with time during the mechanical testing (i.e., isothermal condition).

STRENGTH TESTING

Test method and equipment

A polyaxial load frame¹⁵ has been developed to apply axial and lateral stresses to the cubical salt specimens (Fig. 2). Two pairs of 152 cm long cantilever beams are used to apply the lateral loads in mutually perpendicular directions. The outer end of each beam is pulled down by a dead weight placed on a lower steel bar linking the two opposite beams underneath. The beam inner end is hinged by a pin mounted between vertical bars on each side of the frame. During testing all beams are arranged nearly horizontally, and hence a lateral compressive load results on the specimen placed at the centre of the frame. Using different distances from the pin to the outer weighting point and to the inner loading point, a load magnification of about 17 to 1 is obtained. This loading ratio is also used to determine the lateral deformation of the specimen by monitoring the vertical movement

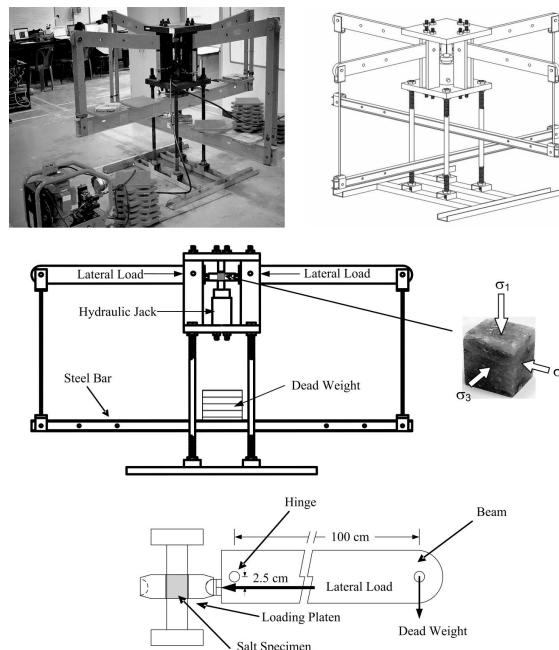


Fig. 2 A polyaxial load frame developed for compressive strength testing of rock salt under various temperatures.

of the two steel bars below. The maximum lateral load is designed for 100 kN. Prior to testing, both lateral loads are calibrated to obtain a desired lateral stress. The calibration is performed by placing an electronic load cell between the opposite cantilever beams. Neoprene sheets have been placed at the interface between loading platens and rock surfaces to minimize the friction. The axial load is applied by a 1000-kN hydraulic load cell connected to an electric oil pump via a pressure regulator.

The frame has an advantage over the conventional triaxial cell because it allows a relatively quick installation of the test specimen under triaxial loading condition, and hence the change of the specimen temperature during testing is minimal.

Test results

Ten specimens have been tested for each temperature level with confining (lateral) stresses of 0, 3, 5, 10, 15, 20, and 30 MPa. They are loaded axially at a constant rate of 1 MPa/s until failure occurs. Fig. 3 shows stress-strain curves monitored from some of the salt specimens under various temperatures and confining pressures. For all specimens, the two measured lateral strains induced by the same magnitude of the applied lateral stresses are similar. Some discrepancies may be due to the intrinsic variability of the salt.

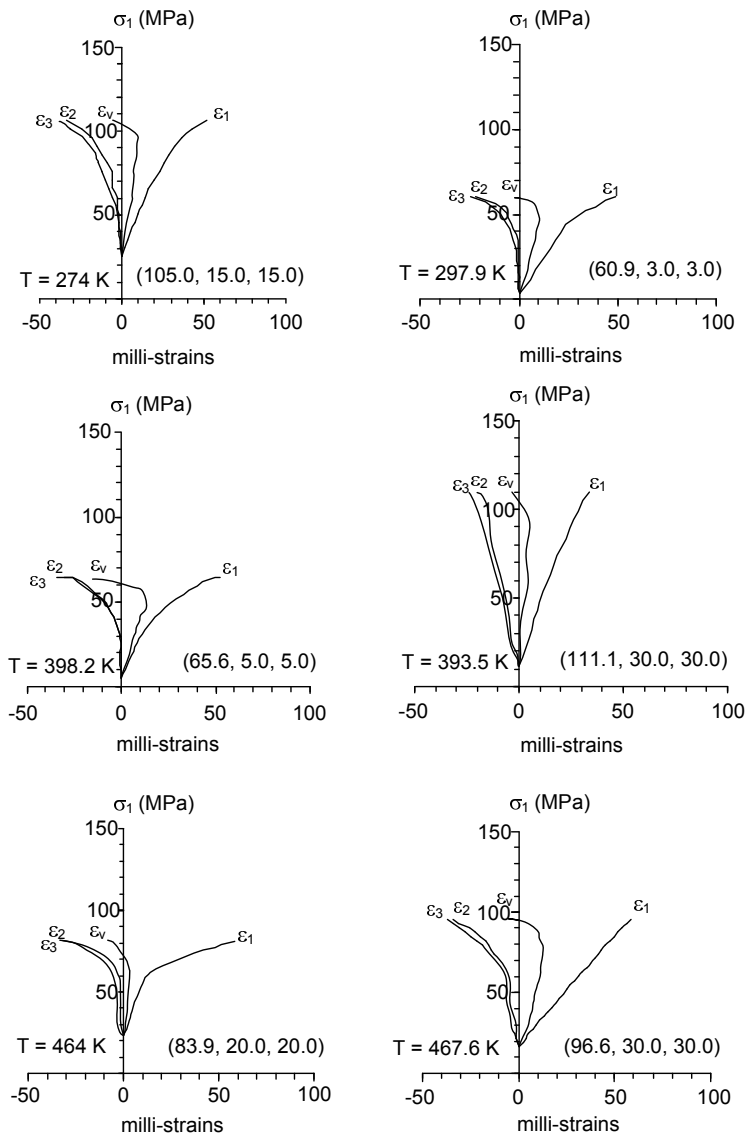


Fig. 3 Stress-strain curves obtained from some salt specimens with different temperatures. Numbers in brackets indicate ($\sigma_1, \sigma_2, \sigma_3$) at failure.

The results indicate that the uniaxial compressive strengths (σ_c) of salt decrease linearly with increasing temperature (T) and can be represented best by (Fig. 4 and Table 1):

$$\sigma_c = -0.067 T + 56.7 \text{ MPa.}$$

Table 2 shows the triaxial compressive strength results. Under the same confining pressure (σ_3), the maximum principal stress at failure (σ_1) decreases with increasing specimen temperature. Some post-test salt specimens are shown in Fig. 5. Most specimens show induced-cracks parallel to the major principal

Table 1 Uniaxial compressive strengths of rock salt.

Specimen no.	ρ (g/cm ³)	T (K)	σ_c (MPa)
UCS 45–47	2.12 ± 0.03	277.0 ± 2.3	37.9 ± 3.0
UCS 81, 87, 90	2.00 ± 0.05	298.0 ± 0.6	37.0 ± 2.5
UCS 51–53	2.10 ± 0.01	394.0 ± 4.7	30.0 ± 3.5
USC 74	2.15	455.5	25

stress direction. No significant difference of the crack patterns in the specimens was obtained under different temperatures and confining pressures.

The Brazilian tensile strength of the salt has been

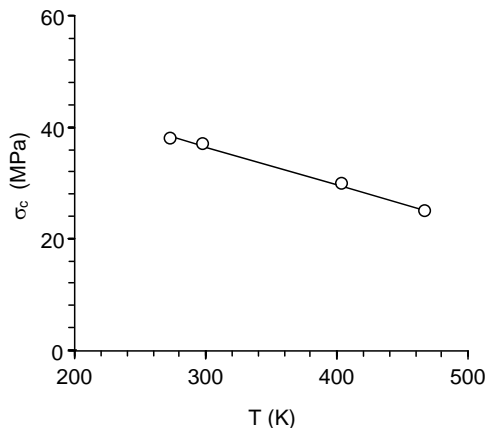


Fig. 4 Uniaxial compressive strength of salt as a function of temperature.

Table 2 Triaxial compressive strengths of rock salt.

σ ₃ (MPa)	σ ₁ (MPa)			
	274 K	280 K	404 K	467 K
1.6	49.0	45.9	–	–
3	63.6	60.9	52.5	–
5	77.9	76.8	65.6	50.0
10	96.6	93.0	80.6	67.4
15	109.5	105.0	88.9	77.1
20	118.6	113.3	96.0	83.9
30	135.0	128.5	111.0	97.1

determined from disk specimens at temperatures of 273, 298, 404, and 467 K. Except for the pre-heating and cooling, the test procedure, sample preparation, and strength calculation follow the ASTM standard practice¹⁶. Table 3 shows the tensile strength results. Some post-test specimens of the Brazilian testing are shown in Fig. 6. The tensile strength (σ_B) decreases linearly with increasing specimen temperature (T), and can be represented by (Fig. 7):

$$\sigma_B = -0.012T + 10.5 \text{ MPa.}$$

The maximum principal stresses at failure (σ₁) from the compressive and tensile testing are presented as a function of the minimum principal stress (σ₃) in

Table 3 Brazilian tensile strengths of rock salt.

Specimen no.	ρ (g/cm ³)	T (K)	σ _B (MPa)
BZ 1–10	2.12 ± 0.01	274.0 ± 3.1	7.3 ± 0.51
BZ 11–20	2.10 ± 0.05	297.5 ± 0.8	6.0 ± 0.60
BZ 21–30	2.21 ± 0.04	393.7 ± 5.1	5.8 ± 0.84
BZ 31–40	2.09 ± 0.04	464.7 ± 4.5	4.8 ± 0.42

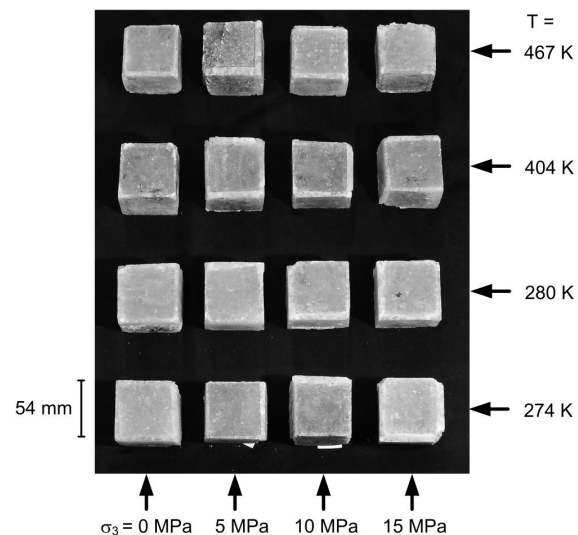


Fig. 5 Some post-test salt specimens from compressive strength testing under different confining pressures (σ₃) and temperatures (T).

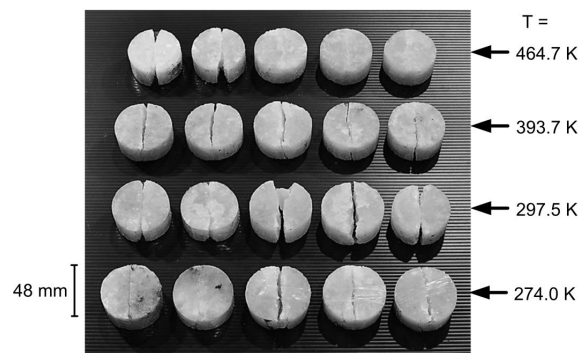


Fig. 6 Some post-test salt specimens from Brazilian tensile strength testing.

Fig. 8. Nonlinear relations were observed at all temperature levels. The higher the temperature imposed on the salt specimen, the lower a failure envelope was obtained.

Based on the Coulomb criterion the cohesion (c) and internal friction angle (φ) can be determined from the strength results for each temperature using the following relations¹⁷:

$$\sigma_1 = \sigma_c + \sigma_3 \tan^2 [(\pi/4) + (\phi/2)],$$

$$\sigma_c = 2c \tan [(\pi/4) + (\phi/2)].$$

They are determined from the tangent of the σ₁–σ₃ curves at σ₃ = 10 MPa. It is found that the cohesion and friction angle decreased linearly with increasing temperature (Fig. 9) which agrees reasonably

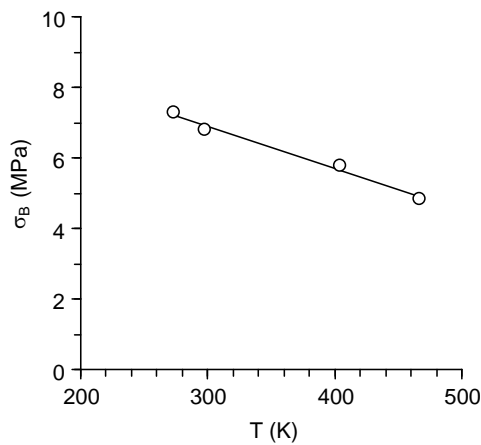


Fig. 7 Brazilian tensile strength of salt as a function of temperature.

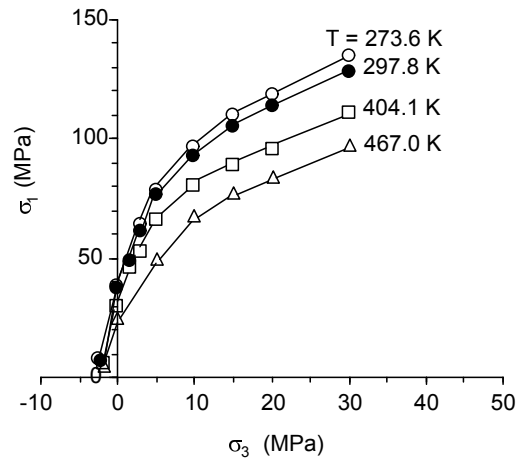


Fig. 8 Major principal stress at failure as a function of confining pressure.

well with the linear drop of the uniaxial and tensile strengths as the temperature increases.

To incorporate the intermediate principal stress (σ_2), the test results can be presented in terms of the octahedral shear stress at failure (τ_{oct}) as a function of mean stress (σ_m), as shown in Fig. 10, where¹⁷:

$$\tau_{oct} = \sqrt{\frac{1}{3} [(\sigma_1 - \sigma_2)^2 + (\sigma_2 - \sigma_3)^2 + (\sigma_3 - \sigma_1)^2]}$$

$$\sigma_m = \frac{1}{3} (\sigma_1 + \sigma_2 + \sigma_3)$$

The diagram in Fig. 10 clearly indicates that the effect of temperature on the salt strength was larger when the salt was under higher confining pressures. When σ_m is below 20 MPa, the octahedral shear strengths for salt were less sensitive to the temperature.

STRAIN ENERGY DENSITY CRITERION

The strain energy density principle is applied here to describe the salt strength and deformability under different temperatures. It is assumed that under a given mean strain energy and temperature the distortional strain energy required to fail the salt specimens is constant. Regression on the test results shows that the distortional strain energy (W_d) increases linearly with the mean strain energy (W_m):

$$W_d = A W_m + B$$

The parameters A and B are empirical parameters depending on the strength and cohesion of the salt under each temperature. They can be determined by regression analysis on the test data (Fig. 11). It is

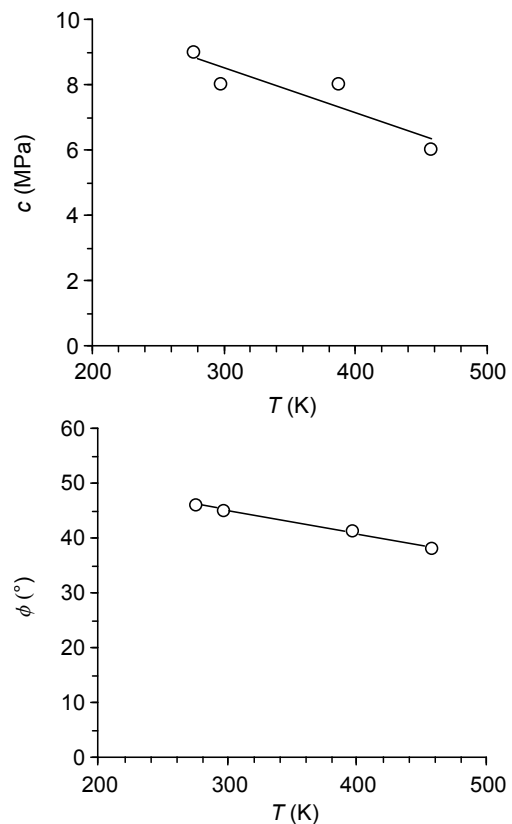


Fig. 9 Cohesion and internal friction angle of salt as a function of temperature.

interesting to note that the rates of the increase of W_d with respect to W_m are virtually the same for all temperature levels.

Assuming that for each temperature level the salt

Table 4 Elastic parameters and strain energy density at failure.

T_{avg} (K)	σ_m (MPa)	τ (MPa)	E (GPa)	ν	G (GPa)	K (GPa)	W_d (MPa)	W_m (MPa)
274	23.2	28.6	27.1	0.38	9.8	37.6	–	–
	29.3	34.4	29.1	0.42	10.2	60.6	–	–
	38.9	40.8	28.7	0.32	10.9	26.6	893.6	700.0
	46.5	44.5	29.1	0.34	10.9	30.3	1368.6	1000.0
	52.9	46.5	27.1	0.37	9.9	34.7	1725.2	1300.0
	65.0	49.5	29.5	0.35	10.9	32.8	2242.2	1600.0
	Mean \pm SD		28.4 \pm 0.9	0.36 \pm 0.04	10.4 \pm 0.4	37.1 \pm 3.2		
298	17.4	22.3	21.0	–	–	–	–	–
	22.3	27.3	27.0	0.35	10.0	30.0	–	–
	28.9	33.8	26.8	0.36	9.9	31.9	935.6	600.0
	37.7	39.1	27.5	0.31	10.5	24.1	1158.5	750.0
	45.0	42.4	24.0	0.34	9.0	24.2	1458.0	970.0
	51.1	44.0	21.5	0.34	8.0	22.4	1944.0	1150.0
	Mean \pm SD		25.5 \pm 2.1	0.34 \pm 0.02	9.5 \pm 0.8	27.8 \pm 4.8	2292.0	1500.0
404	16.4	20.9	18.7	–	–	–	–	–
	19.5	23.3	20.1	0.36	7.4	23.9	–	–
	25.2	28.6	22.3	0.42	8.1	31.0	940.4	413.5
	33.5	33.3	19.8	0.41	7.0	36.7	1479.6	800.0
	39.6	34.8	17.5	0.30	6.6	17.2	1779.4	979.3
	45.3	35.8	20.9	0.32	7.9	19.4	2100.0	1100.0
	Mean \pm SD		20.0 \pm 1.5	0.37 \pm 0.05	7.5 \pm 0.5	25.3 \pm 7.3	2300.0	1300.0
467	20.0	21.2	17.5	0.36	6.4	20.8	935.6	350.0
	29.1	27.1	16.2	0.34	6.0	16.9	1158.5	400.0
	35.7	29.3	18.5	0.40	6.6	30.8	1458.0	650.0
	41.3	30.1	20.0	0.36	7.4	23.8	1944.0	955.0
	52.4	31.6	17.3	0.34	6.5	18.0	2292.0	1132.0
		Mean \pm SD		18.1 \pm 1.4	0.36 \pm 0.02	6.6 \pm 0.5	22.1 \pm 5.6	

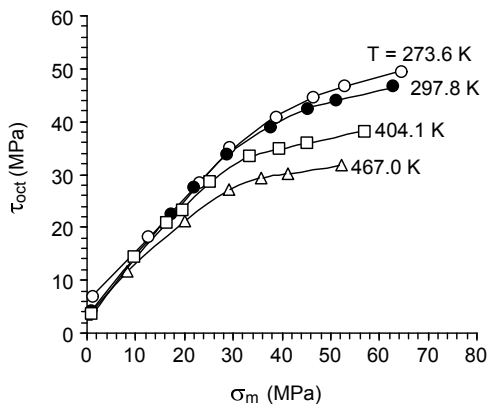


Fig. 10 Octahedral shear strength of salt as a function of mean stress.

is linearly elastic prior to failure, W_d and W_m can be determined for each specimen using the following relations¹²:

$$W_d = \frac{3}{4} \left(\frac{\tau_{oct}^2}{G} \right) \quad (1)$$

$$W_m = \left(\frac{\sigma_m^2}{2K} \right) \quad (2)$$

The elastic parameters G and K can be defined as a function of the testing temperature, and hence the salt strengths from different temperatures can be cor-

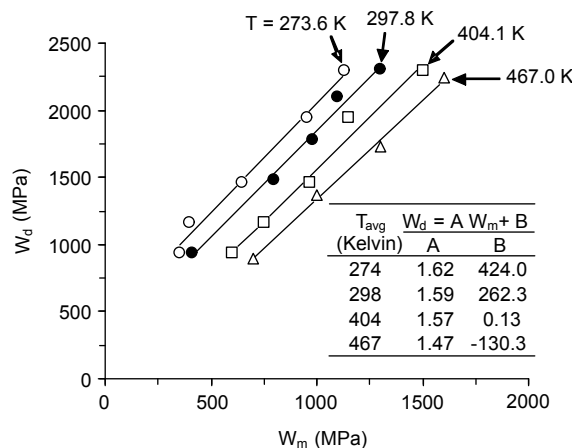


Fig. 11 Distortional strain energy at failure as a function of mean strain energy.

related. **Table 4** summarizes the measurement results for each specimen in terms of the elastic modulus (E), shear modulus (G), bulk modulus (K), and Poisson's ratio (ν). Linear variations of the four parameters with respect to temperature are observed (**Fig. 12**). Good correlations (coefficient of correlation greater than 0.9) are obtained when they are fitted with the

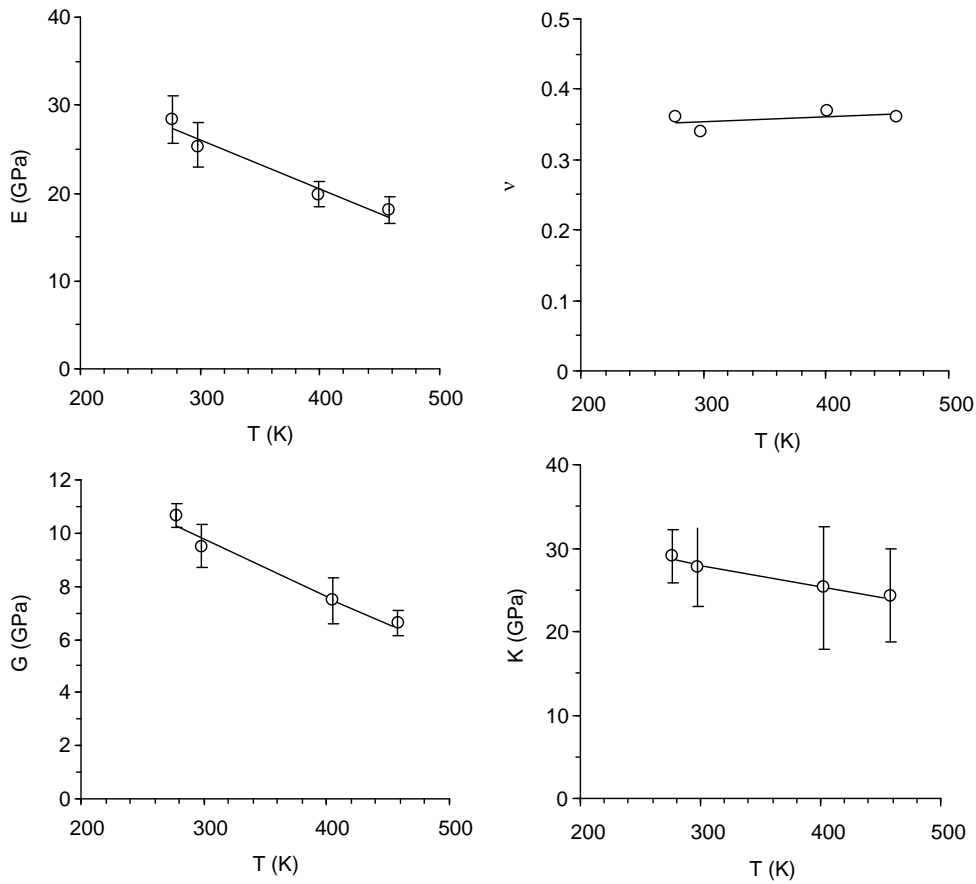


Fig. 12 Elastic parameters of salt as a function of temperature.

following linear equations:

$$E = -0.06 T + 42.7 \text{ GPa} \quad (3)$$

$$G = -0.0215 T + 16.2 \text{ GPa} \quad (4)$$

$$K = -0.0254 T + 35.6 \text{ GPa} \quad (5)$$

$$\nu = (7 \times 10^{-6}) T + 0.33 \quad (6)$$

The results indicate that the elastic, shear, and bulk moduli decrease with increasing temperature. Poisson's ratio however tends to be independent of the temperature. By substituting (4) into (1) and (5) into (2) the W_d at failure can therefore incorporate the effect of temperature into the strength calculation.

The distortional strain energy for each salt specimen at failure, that implicitly takes the temperature effect into consideration, is plotted as a function of the mean strain energy in Fig. 13. The data can be described best by a linear equation:

$$W_d = A_{Th} W_m + B_{Th} \quad (7)$$

The parameters A_{Th} and B_{Th} are empirical constants depending on the strength and thermal response

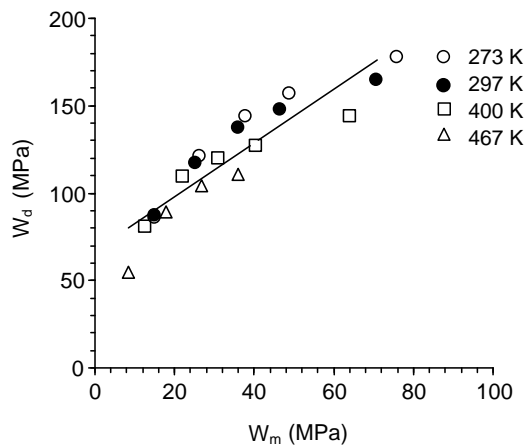


Fig. 13 Distortional strain energy as a function of mean strain energy.

of the rock. For the Maha Sarakham salt $A_{Th} = 1.53$ and $B_{Th} = 63.7 \text{ MPa}$. A good correlation is obtained between the test results and the proposed criterion

($R^2 = 0.851$).

DISCUSSION AND CONCLUSIONS

This study experimentally determines salt strengths under different temperatures ranging of 273, 298, 404, and 467 K (0–194 °C). This range of testing temperatures is selected to cover those likely occurred around the storage caverns under operation and to obtain a rigorous relationship between the temperatures and strengths of the salt. During injection period, the storage cavern may be subject to temperatures as high as 140 °C (414 K), depending on the injection rate and maximum storage volume and pressure⁷.

For each temperature the testing is assumed to be under isothermal condition (constant temperature with time during loading). For this simplified approach the salt specimens subject to different temperatures have been taken as different materials. As a result, the induced thermal stress or thermal energy imposed on the salt specimens has not been explicitly incorporated into the initial strength calculation. Although this approach differs from the complex thermo-mechanical analysis, it provides a quick assessment of the cavern stability when the surrounding salt is under elevated temperatures.

The decrease of the salt strength as the temperature increases suggests that the applied thermal energy before the mechanical testing makes the salt weaker, and more plastic—failing at lower stress and higher strain with lower elastic and shear moduli. The temperature effect is larger when salt is under higher mean stress. To determine the temperature dependency of the failure stress and strain and elastic properties, the strain energy density concept is applied. Assuming that the salt is linearly elastic before failure, the distortional strain energy (W_d) at failure can be calculated as a function of mean strain energy, W_m (Fig. 11). For a given W_m , the W_d decreases with increasing temperature. The differences of W_d from one temperature to the other therefore correspond to the difference of thermal energy imposed on the specimens.

The single multi-axial strength criterion (7) for salt under various confining pressures and temperatures implicitly considers the effect of the thermal energy by incorporating empirical equations between the elastic parameters and temperature into the W_d – W_m relation (Fig. 12). The strain energy criterion agrees well with the strength results from different temperature levels (Fig. 13). Since the analysis is intended to determine the short-term strength, the creep deformations induced by the mechanical and thermal loadings are not considered here.

The proposed criterion can be used to determine the stability of rock salt around compressed-air or gas storage caverns during product injection (high temperature, low deviatoric stress) and withdrawal (low temperature, high deviatoric stress). The effect of temperature on the salt strength may be enhanced for the salt cavern with high frequency of injection-retrieval cycles. To be conservative, the maximum temperature (induced during injection) and the maximum shear stresses (induced during withdrawal) in salt around the cavern should be determined (normally by numerical simulation). The salt stability can be determined by comparing the computed temperature distribution and mechanical and thermal stresses against the criterion proposed above. The results should lead to a conservative design of the safe maximum and minimum storage pressures.

Acknowledgements: This study is funded by Suranaree University of Technology. Permission to publish this paper is gratefully acknowledged. We would like to thank Asean Potash Mining Co. for donating salt cores for testing.

REFERENCES

1. Vosteen H, Schellschmidt R (2003) Influence of temperature on thermal conductivity, thermal capacity and thermal diffusivity for different types of rock. *Phys Chem Earth* **28**, 499–509.
2. Shimada M, Liu J (2000) Temperature dependence of strength of rock under high confining pressure. *Annuals Disas Prev Res Inst* **43B-1**, 75–84.
3. Okatov RP, Nizametdinov FK, Tsai BN, Bondarenko TT (2003) Time and temperature factors in construction of rock strength criteria. *J Min Sci* **39**, 139–42.
4. Hansen FD, Carter NL (1980) Creep of rock salt at elevated temperature. In Summers DA (ed) *Proceedings of the 21st U.S. Symposium on Rock Mechanics*, Univ of Missouri, Rolla, pp 217–26.
5. Liang WG, Xu SG, Zhao YS (2006) Experimental study of temperature effects on physical and mechanical characteristics of salt rock. *Rock Mech Rock Eng* **39**, 469–82.
6. Duddeck HW, Nipp HK (1982) Time and temperature dependent stress and displacement fields in salt domes. In *Proceedings of the 23rd Symposium on Rock Mechanics*, Berkeley Publ, New York: AIME.
7. Katz DLV, Lady ER (1976) *Compressed Air Storage for Electric Power Generation*, Malloy Lithographing Inc., Michigan.
8. Gronefeld P (1989) Thermodynamic behavior of HP natural gas caverns in salt—Theoretical calculations and practical experience. In *Proceedings of the International Conference on Storage of Gases in Rock Caverns*, Trondheim, A.A. Balkema, Rotterdam, pp 121–7.

9. Jeremic ML (1994) *Rock Mechanics in Salt Mining*, A.A. Balkema, Rotterdam.
10. Warren J (1999) *Evaporites: Their Evolution and Economics*, Blackwell Science, Oxford.
11. Fuenkajorn K, Archeeploha S (2009) Prediction of salt cavern configurations from subsidence data. *Eng Geol* **110**, 21–9.
12. Fuenkajorn K, Phueakphum D (2010) Effects of cyclic loading on mechanical properties of Maha Sarakham salt. *Eng Geol* **112**, 43–52.
13. Suwanich P (1978) Potash in Northeastern of Thailand. Economic Geology Document. Vol. 22. Economic Geology Division, Department of Mineral Resources, Bangkok.
14. Tabakh ME, Utha-Aroon C, Schreiber BC (1999) Sedimentology of the Cretaceous Maha Sarakham evaporates in the Khorat Plateau of northeastern Thailand. *Sediment Geol* **123**, 31–62.
15. Sriapai T, Samsri P, Fuenkajorn K (2011) Polyaxial strength of Maha Sarakham salt. In: Fuenkajorn K, Phien-wej N (eds) *Proceedings of The 3rd Thailand Symposium on Rock Mechanics (ThaiRock 2011)*, Suranaree Univ of Technology, Nakhon Ratchasima, Thailand, pp 79–87.
16. ASTM D3967-08 (2008) Standard test method for splitting tensile strength of intact rock core specimens. *Annual Book of ASTM Standards*, Vol. 04.08, West Conshohocken, PA: ASTM.
17. Jaeger JC, Cook NGW, Zimmerman RW (2007) *Fundamentals of Rock Mechanics*, 4th edn, Blackwell Publishing, Oxford.